Introduction of Two Novel Stiffness Parameters and Interpretation of Air Puff Induced Biomechanical Deformation Parameters with a Dynamic Scheimpflug Analyzer

Cynthia J. Roberts, PhD[1]; Ashraf M. Mahmoud, BS[1]; Jeffrey P. Bons, PhD[2]; Arif Hossain, MS[2]; Ahmed Elsheikh, PhD[3-4]; Riccardo Vinciguerra, MD[5]; Paolo Vinciguerra, MD[6-7]; Renato Ambrósio Jr, MD, PhD[8-9]

Affiliations:

[1]Department of Ophthalmology & Visual Science, and Department of Biomedical Engineering, The Ohio State University, Columbus, OH, USA; [2]Department of Mechanical & Aerospace Engineering, The Ohio State University, Columbus, OH USA; [3]School of Engineering, University of Liverpool, Liverpool, United Kingdom; [4]NIHR Biomedical Research Centre for Ophthalmology, Moorfields Eye Hospital NHS Foundation Trust and UCL Institute of Ophthalmology, United Kingdom; [5]Department of Surgical Sciences, Division of Ophthalmology, University of Insubria, Varese, Italy; [6]Eye Center, Humanitas Clinical and Research Center, Via Manzoni 56, Rozzano (MI) – Italy; [7]Vincieye Clinic, Milan, Italy; [8]Rio de Janeiro Corneal Tomography and Biomechanics Study Group – Rio de Janeiro, Brazil; [9]Department of Ophthalmology, Federal University of São Paulo – São Paulo, Brazil

Corresponding author:

Dr Cynthia Roberts, Department of Ophthalmology & Visual Science, The Ohio State University, 915 Olentangy River Road, Suite 5000, Columbus, OH, 43220 Email: Roberts.8@osu.edu; Phone: 614-293-7039

Financial Disclosures:

Financial Disclosure(s): Dr. Ambrósio, Dr. Vinciguerra, and Dr. Roberts are consultants for OCULUS Optikgeräte GmbH. Dr. Elsheikh has received research funding from OCULUS Optikgeräte GmbH. None of the remaining authors have any financial disclosures.

Running head

Relationship between Deformation Response Parameters and New Stiffness Parameters

PRECIS

Introduction of two novel stiffness parameters will allow interpretation of dynamic corneal response parameters of a Dynamic Scheimpflug Analyzer, regarding resistance to deformation.

Abstract

Purpose: To investigate two new stiffness parameters (SPs), and compare between normal (NL) and keratoconic (KC) eyes.

Methods: SPs are defined as Resultant Pressure at inward applanation (A1), divided by corneal displacement. SP-A1 uses displacement between the undeformed cornea and A1; SP-HC from A1 to maximum deflection during highest concavity (HC). The spatial and temporal profiles of the Corvis ST air puff were characterized using hot wire anemometry. An adjusted air pressure impinging on the cornea at A1 (adjAP1), and an algorithm to biomechanically correct IOP based on finite element modelling (bIOP), were used for Resultant Pressure calculation (adjAP1 - bIOP). Linear regression analyses between dynamic corneal response parameters (DCR's) and SPs were performed on a retrospective dataset of 180 KC eyes and 482 NL eyes. DCR's from a subset of 158 eyes of 158 subjects in each group were matched for bIOP and compared using t-tests. Significance threshold was $p < 0.05$.

Results:

All DCR's evaluated showed significant differences between NL and KC, except peak distance. KC eyes had lower SP values, thinner pachymetry, shorter applanation lengths, greater absolute values of applanation velocities, earlier A1 times and later second applanation times, greater highest concavity (HC) deformation amplitudes and HC deflection amplitudes, and lower HC radius of concave curvature (greater concave curvature). Most DCR's showed a significant relationship with both SPs in both groups.

Conclusions: Keratoconic eyes demonstrated less resistance to deformation than normal eyes with similar IOP. The SPs may be useful in future biomechanical studies as potential biomarkers.

The importance of corneal biomechanics in ophthalmology has fueled the drive to develop new devices for the clinical assessment of corneal biomechanical properties, as well as compensate for the influence of biomechanical properties on estimation of intraocular pressure (IOP). [1] Historically, assessment of corneal stiffness has been accomplished via cutting strips of corneal tissue from post-mortem donors, and applying a tensile load in the form of stretching the tissue to specific strains, defined as percent change in length, while plotting the stress at each level of strain. [2-5] The slope of the stress-strain curve is defined as the tensile elastic modulus, with greater slope indicating a higher elastic modulus and a stiffer material. This can also be interpreted that a stiffer material has greater resistance to deformation, since a higher stress is associated with a lower strain than in a softer material. The evaluation is more complicated in a cornea since it is viscoelastic in nature, which means that the stress-strain response is a function of the strain rate, or how quickly the tissue is stretched, [6] as well as exhibiting a nonlinear stress-strain relationship such that higher levels of stress are associated with greater elastic modulus. [6,7] The challenge in transferring biomechanical property assessment to the in vivo condition has been to determine a clinically acceptable approach to perturb a cornea that is preloaded by IOP, as well as to manage eye motion. Since biomechanical properties are defined by the response to a perturbation or applied load, a clinically viable load must be determined. In addition, IOP is a confounding factor in assessment of corneal biomechanics, since the cornea stiffens as IOP increases, making the two factors of stiffness and IOP inseparable. [8]

The first clinical device to be introduced capable of assessing biomechanics was the Ocular Response Analyzer (ORA), [9] followed by the Corvis ST. [10] Both current clinical devices rely on an air puff to deform the cornea and assess biomechanical deformation response

parameters. The ORA relies on an indirect assessment of deformation response and produces corneal hysteresis (CH) which is widely recognized as a biomechanical parameter, but which is complicated to interpret due to the nature of the measurement. The Corvis ST uses ultra high-speed Scheimpflug imaging to directly assess deformation response. This allows visualization and analysis of a large set of biomechanical deformation response parameters. However, interpretation of the data produced is difficult due to the quantity of parameters and their interaction with both stiffness and IOP. Therefore, the purpose of the current study is to define two new stiffness parameters that are a function of IOP, and investigate the relationship of various dynamic corneal response parameters (DCR's) to these global indications of corneal stiffness, in both normal subjects and those diagnosed with keratoconus.

Methods

Subjects and Devices

A retrospective study was conducted with subjects enrolled from two sites: the *Instituto de Olhos Renato Ambrósio* in Rio de Janeiro, Brazil, and the Vincieye Clinic in Milan, Italy. For each subject, a random eye was chosen for inclusion in the study. The combined dataset consisted of 180 eyes of 180 keratoconic (KC) subjects, diagnosed by RA or PV, respectively, as well as 482 eyes of 482 normal (NL) subjects. All subjects had received a complete ophthalmic examination that included the CorVis ST and Pentacam (OCULUS Optikgeräte GmbH, Wetzlar, Germany). The Corvis ST is a Dynamic Scheimpflug Analyzer which uses a consistent air puff to deform the cornea while an ultra-high speed camera (~4,300 frames per second) utilizing Scheimpflug geometry, simultaneously captures a series of 140 images of a single, central, horizontal meridian of the cornea.

The inclusion criteria for the keratoconic population included the presence of a bilateral clear topographic and tomographic keratoconus without any previous ocular surgeries, such as corneal collagen cross linking or implanted intracorneal rings. Conversely, the inclusion criteria for the healthy subjects included the presence of a Corvis ST exam in the database, a Belin Ambrósio Enhanced Ectasia Index total deviation (BAD-D) from the Pentacam less than 1.6 standard deviations (SD) from normative values in both eyes. Exclusion criteria were any previous ocular surgery or disease, myopia over 10D and any concomitant or previous glaucoma or hypotonic therapies. The BAD-D cut off of 1.6 SD was used because it is described as the best performing screening parameter with values of 1.65 and 1.88 associated with a 95% and 97.5% confidence interval, respectively, with an acceptable false negative rate of less than 1%. [11] Only Corvis ST exams with quality score "OK" were included in the analysis, and Research Software was used. Additionally, a second manual, frame-by-frame analysis of the exam, made by an independent masked examiner, was performed to ensure quality of each acquisition. The main criterion was good edge detection over the whole deformation response, with the exclusion of alignment errors (x-direction). Similarly, blinking errors were omitted. Moreover, all exams of the Vincieye Clinic were re-evaluated by a masked expert of Anterior Segment (R. Ambrósio) to confirm the diagnosis. Similarly, all the exams of the *Instituto de Olhos Renato Ambrósio* were re-evaluated by a masked expert (P Vinciguerra). All measurements with the Corvis ST were taken by the same experienced technicians.

Demographic data, including age and sex, were also acquired. In Brazil, the local Institutional Review Board approved the study and determined that patient consent was not required. In Italy, the local Institutional Review Board determined that approval was not required. However, subjects provided informed consent to provide their data for research at the

time they were seen in clinic. The study was conducted according to the 1964 Declaration of Helsinki, as revised in 2000. All data were exported from the respective device at each site, and transferred to The Ohio State University for further analysis after anonymization.

A description of the phases in the Corneal Deformation Process and associated DCRs is given in the Supplemental Materials.

Stiffness Parameter and IOP

Conceptually, stiffness describes the resistance to deformation. Therefore, with the goal to develop simple clinical parameters that would correlate with stiffness, two novel stiffness parameters (SP) were developed, defined as Resultant Pressure (Pr) divided by displacement. The position of first applanation (A1) was the reference for calculating the load on the cornea, Pr. SP-A1 uses the displacement between the apex in the undeformed state and the deflection at A1 (A1DeflAmp). SP-HC uses the difference in A1 position and maximum deflection near highest concavity (HC): (DeflAmpMax) minus deflection amplitude at A1 (A1DeflAmp). Resultant pressure was calculated as the air pressure impinging on the cornea at the time of applanation minus the IOP. To determine the air pressure on the cornea, the spatial and temporal profiles of the air puff were measured by hot wire anemometry in the xy and xz planes, shown in Figure 1A. A photocell sensor was installed at the outlet of the nozzle to synchronize measured velocity data and the pressure signal produced by the Corvis ST. Hot wire calibration was done with a 2.5mm orifice in order to replicate the actual flow condition in the subsequent experiments. Data were acquired at a sampling rate of 20kHz, from 0 to 16mm from the nozzle in 2mm increments in the axial direction and in .75mm increments up to 3mm on each side of the centerline, for a total of 81 individual points, shown in Figure 1B, with 40 individual puffs for

each data point. The characterization of the air puff demonstrated that the velocity time history at a single location remained consistent for all 40 puffs that were measured, and the flow was also verified to be axisymmetric. This velocity was converted to a dynamic pressure using the ambient density.

For each clinical exam, pressure at first applanation (AP1) was used to align with the time-synchronized measured velocity and pressure signals, shown in Figure 2A. From this, the velocities at z positions of 10mm and 12mm from the nozzle were determined, corresponding to the phase-adjusted time of AP1. The z position of the corneal surface within the image window at A1 was exported from the Corvis ST and the total distance from the nozzle was calculated. This value was used to interpolate between the 10mm and 12mm positions on the centerline velocity distribution, Figure 2B. Prior to interpolation, each curve was fit with a polynomial in the region of A1, approximately 6ms to 14ms. The order of the polynomial was increased until a maximum R^2 resulted, which was a cubic at 10mm and 4^{th} order at 12mm, for an R^2 of .9998. This interpolated velocity for each exam, along with the z position of the cornea at the time of inward applanation, was used to calculate the adjusted air pressure value (adjAP1) at the time and position of A1. An algorithm intended to produce an IOP estimate that compensates for the effects of central corneal thickness (CCT), and age has been developed numerically using finite element analysis, and validated both experimentally and clinically.[12] This algorithm, modified with Corvis ST data to produce a biomechanically-corrected IOP estimate (bIOP), was used to generate the IOP value in both stiffness parameter calculations, with the final equations:

SP-A1 = (adjAP1 - bIOP)/ (A1DeflAmp); and

SP-HC = (adjAP1 - bIOP)/ (DeflAmpMax – A1DeflAmp).

These values take into account both the intraocular pressure and pure corneal deflection, both of which have confounded earlier analyses of corneal deformation parameters.

Statistical Analysis

In order to determine the influence of stiffness on corneal deformation parameters, a series of regression analyses were performed with SP-A1 or SP-HC as the independent variable and each deformation parameter as the dependent variable for both the normal and keratoconic groups. In order to compare deformation parameters between groups, a subset of 158 normal and 158 keratoconic subjects were matched by bIOP, and t-tests were performed on the corneal deformation parameters between groups, with a significance threshold of $p < 0.05$. In order to investigate timing of the maximum difference in deformation of the corneal apex divided by the average deformation 2mm from either side of the apex (DA Ratio) and the timing of maximum whole eye motion (WEMmax), two regression analyses were performed, including the time of DA ratio vs A1 time, as well as the time of WEMmax vs A2 time. In addition, to test the prediction that the difference in arclength between highest concavity (HC) and the predeformation arclength (HCdarclength) is a function of corneal deflection amplitude at highest concavity (HCDeflAmp), a third regression analysis was performed between HCdarclength and HCDeflAmp.

Results

Regression analysis of A1 time and DA Ratio time showed a significant positive linear relationship between the two for both normal and keratoconic subjects (NL: $R^2 = .8164$, $p < .0001$; KC: $R^2 = .6749$, $p < .0001$). The relationship between A2 time and the time of WEMmax

is also a significantly positive linear relationship in both groups (NL: R^2 = .0392, p< .0001; KC: R^2 = .0352, p = .0117). However, the R^2 is substantially lower than the first comparison, meaning not only greater variability, but also a much weaker correlation between A2 time and the time of WEMmax. Finally, the relationship between HCDeflAmp and HCdarclength (a negative number) is significantly negative for normal eyes, meaning that higher HC deflection amplitude is associated with greater change in arclength (a larger magnitude negative value), which is expected. However, it is significantly positive for keratoconic eyes, which is opposite to that of normal eyes and unexpected (NL: R^2 = .2627, p< .0001; KC: R^2 = .0307, p < .0185). See Figure 3.

The comparison of DCRs in the bIOP-matched subset of normal and keratoconic subjects is given in Table 1, and indicates significant differences of all reported parameters, except peak distance which is the width of the concavity at HC, with normal eyes exhibiting stiffer behavior, or less resistance to deformation, than keratoconic eyes for all other parameters. The normal group is stiffer with greater SP-A1 and SP-HC, thicker pachymetry, lower DA Ratio, later A1 times (requiring higher air pressure) with longer applanation lengths and slower velocities, lower deformation and deflection amplitudes, greater HC radius (flatter curvature) with lower Inverse Radius, and earlier A2 times with greater whole eye motion.

The results of the regression analyses are summarized in Tables 2 and 3 for SP-A1 and SP-HC, respectively. Selected regression plots are shown in Figures 4-7. In both normal and keratoconic subjects, both stiffness parameters are significantly positively correlated with second applanation length, first applanation time, HCRadius, pachymetry, and IOP; as well as

significantly negatively correlated with absolute magnitude of both applanation velocities, second applanation time, both DA and DA Ratio, HCDeflAmp, HCDeflArea, Peak Distance, and InvRadMax. SP-A1 was significantly positively correlated with A1 Length and significantly negatively correlated with A1DeflAmp only in Keratoconic eyes, and no relationship in either group with WEM. SP-HC was significantly positively correlated with Al Length in both groups, though weak, and both A1DeflAmp and Whole Eye Motion were correlated only in normal eyes. The relationship of WEM in keratoconic eyes was not significant for SP-HC. For HCdarclength, both SP-A1 and SP-HC were significantly positively correlated in normal eyes and significantly negatively correlated in keratoconic eyes, though both relationships were weak.

Discussion

Biomechanical response parameters can be interpreted relative to stiffness in terms of resistance to deformation. The stiffer the cornea, the greater is the resistance to deformation, and therefore greater air pressure is required to initiate and maintain motion. The major confounding factor is IOP, since both the cornea and sclera will stiffen as IOP increases. [8] This is due to two factors in combination: 1) LaPlace's Law which states that as internal pressure increases, wall stress also increases; and 2) the nonlinear properties of the cornea such that as stress increases, the elastic modulus, E, also increases. This leads to a complex corneal response to air puff induced deformation in the intact globe. Certain response parameters will be dominated by IOP, whereas others will be dominated by corneal stiffness. [13] However, the entire response will be integrated over all influencing factors. In the current study, the confounding influence of IOP was removed in the comparison of normal corneas to those with keratoconus by matching both groups on bIOP. With the consistency of the air puff pressure provided by the device under

study validated during characterization, a direct comparison of the response parameters between the two groups can be performed with confidence in this matched subset. **Additional interpretation of the influence of the stiffness parameters on the DCRs is given in the Supplemental Materials.**

The differences between the two stiffness parameters include stronger correlations of both the HC deformation parameters and A2 parameters to SP-HC, than to SP-A1. However, SP-A1 has greater separation between NL and KC groups, shown in Table 1 and illustrated in Figures 4-7. SP-A1 also has stronger correlations to both pachymetry and DA Ratio, which occurs near A1. Therefore, it might be expected that SP-A1 would be a stronger biomarker for corneal conditions, such as keratoconus, and this has been reported. [14] It is expected that SP-HC might be a stronger biomarker for conditions that involve the sclera, since a stiffer sclera can limit the magnitude of maximum corneal deformation. [15] The relationships to A1DeflAmp are interesting in that with SP-HC, a positive correlation exists for the normal eyes, but no significant relationship exits in keratoconus. Conversely, there is no relationship in normal eyes in the regression of A1DeflAmp to SP-A1, but a significant negative correlation exists in keratoconic eyes. For SP-HC, this may be due to corneal geometry near the beginning of the pulse, so that the later applanation time in normal eyes will lead to greater air pressure and greater amplitude at applanation. However, in the comparison between the bIOP-matched groups, A1DeflAmp was lower in the normal eyes than keratoconic eyes. This may be due to greater curvature in keratoconus, which would impact early deflection amplitude, and can also explain the negative correlation in keratoconic eyes to SP-A1. The keratoconic eyes that are

relatively stiffer (less severe disease) would presumably have lower curvature and thus, less amplitude at A1.

The parameter, HCdarclength, showed a different relationship with stiffness between normal and keratoconic eyes, with a significantly positive relationship in NL eyes and significantly negative relationship in KC eyes for both SP-A1 and SP-HC. This can be interpreted that the stiffer the normal eye, the lower the negative change. In other words, with greater resistance to deformation, the arclength shortened less. This was confirmed in the regression between HCdarclength and HCDeflAmp (Figure 3) in normal eyes. As the cornea becomes concave, the arclength shortens with increased crimping of the collagen fibers. Therefore, the greater the amplitude of deflection, the shorter becomes the arclength, or in other words, the greater is the negative change in the HCdarclength in the less stiff normal eyes. However, in keratoconus, the relationship was the opposite in both comparisons, which seems paradoxical. One explaination to consider, however, is the biomechanical consequences of the pathology in the collagen fibers. [16] Ultrastructural abnormalities have been identified in keratoconus, including disorganized collagen fibers [17] with a loss of anchoring fibrils near Bowman's layer,[18]. It may be that the diseased collagen fibers are not able to crimp in the way that normal fibers do. This is consistent with the results of the bIOP-matched comparison, which showed a greater negative HCdarclength in normal eyes than in keratoconus, despite the greater stiffness and resistance to deformation in the normal eyes, combined with lower HCDeflAmp.

In conclusion, two novel stiffness parameters are introduced to allow interpretation of the corneal deformation parameters produced by a Dynamic Scheimpflug Analyzer, relating to how

each parameter responds as corneal and scleral resistance to deformation is increased. Normal eyes show overall greater resistance to deformation than keratoconic eyes. Most DCRs investigated demonstrated a significant relationship to the novel stiffness parameters in normal and keratoconic eyes, based on both pure corneal deflection, as well as deformation amplitude which includes whole eye motion. Keratoconic eyes also showed greater variability in the response parameters, likely due to variability of the disease process. Future research will focus on the clinical utility of the new stiffness parameters as potential biomarkers for pathology. It is reported that SP-A1 has greater clinical utility in corneal conditions, [14] and it is predicted that SP-HC will have greater clinical utility in conditions involving the sclera, such as glaucoma.

References

1. Liu J, Roberts CJ. Influence of corneal biomechanical properties on intraocular pressure measurement: Quantitative analysis. *J Cataract Refract Surg.* 2005; 31:146-155.
2. Andreassen TT, Simonsen AH, Oxlund H. Biomechanical properties of keratoconus and normal corneas. Exp Eye Res 1980; 31:435–44.
3. Nash IS, Greene PR, Foster CS. Comparison of mechanical properties of keratoconus and normal corneas. Exp Eye Res 1982; 35:413–424.
4. Jue B, Maurice DM. The mechanical properties of the rabbit and human cornea. J Biomech 1986;19:847-853.
5. Hoeltzel DA, Altman P, Buzard K, Choe K. Strip extensiometry for comparison of the mechanical response of bovine, rabbit, and human corneas. J Biomech Eng 2002; 114:202–215.
6. Elsheikh A, Wang D, Brown M, Rama P, Campanelli M, Pye D. Assessment of corneal biomechanical properties and their variation with age. Curr Eye Res 2007; 32:11-9.
7. Woo SL, Kobayashi AS, Schlegel WA, Lawrence C. Nonlinear material properties of intact cornea and sclera. Exp Eye Res 1972; 14:29-39.
8. Roberts CJ. Concepts and Misconceptions in Corneal Biomechanics. *J Cataract Refract Surg* 2014;40:862-869.
9. Luce, DA. Determining in vivo biomechanical properties of the cornea with an ocular response analyzer. J Cataract Refract Surg. 2005;31:156-62.
10. Ambrósio Jr R, Ramos I, Luz A, Faria-Correia F, Steinmueller A, Krug M, Belin MW, Roberts C. Dynamic Ultra-High-Speed Scheimpflug imaging for assessing corneal biomechanical properties. Rev Bras. Oftalmol 2013, 72(2):99-102.
11. Villavicencio OF GF, Henriquez MA, Izquierdo L Jr, Ambrosio RR Jr, Belin MW. Independent Population Validation of the Belin/Ambrosio Enhanced Ectasia Display: Implications for Keratoconus Studies and Screening. Int J Kerat Ect Cor Dis 2014;3:1-8.
12. Joda AA, Shervin MMS, Kook D, Elsheikh A. Development and validation of a correction equation for Corvis tonometry. Computer Methods in Biomechanics and Biomedical Engineering 2015; 1-11.
13. Vinciguerra R, Elsheikh A, Roberts CJ, Ambrósio Jr R, Kang DYK, Morenghi E, Azzolini C, Vinciguerra P. Influence of Pachymetry and Intraocular Pressure on Dynamic Corneal Response Parameters. J Refract Surg 2016; 32:550-561.
14. Vinciguerra R; Ambrósio Jr R, Elsheikh A; Roberts CJ, Lopes B, Morenghi E, Azzolini C, Paolo Vinciguerra P. Dectection of Keratoconus with a new Corvis ST Biomechanical Index. *J Refract Surg* 2016; in press.
15. Metzler K, Mahmoud AM, Liu J, Roberts CJ. Deformation Response of Paired Donor Corneas to An Air Puff: Intact Whole Globe vs Mounted Corneoscleral Rim. J Cataract Refr Surg 2014;40(6):888-96
16. Roberts CJ, Dupps, JR. WJ. Biomechanics of Corneal Ectasia and Biomechanical Treatments. J Cataract Refract Surg 2014; 40:991-998.
17. Meek KM, Tuft SJ, Huang Y, Gill PS, Hayes S, Newton RH, Bron AJ. Changes in collagen orientation and distribution in keratoconus corneas. Invest Ophthalmol Vis Sci 2005; 46:1948–56.
18. Morishige N, Wahlert AJ, Kenney MC, Brown DJ, Kawamoto K, Chikama T-i, Nishida T, Jester JV. Second-harmonic imaging microscopy of normal human and keratoconus cornea. Invest Ophthalmol Vis Sci 2007; 48:1087–1094.

Table 1: Mean ± Standard Deviation in IOP_{FEM}-Matched t-test Comparison

N=158 in NL and KC	**Normal**	**Keratoconus**	**P value**
age	40 ± 16	35 ± 12	p =.0028
Pachymetry (μm)	542 ± 34	471 ± 36	< .0001
1st Applanation Length (A1 Length) (mm)	1.82 ± .08	1.72 ± .16	< .0001
1st Applanation Velocity (A1 Vel)(mm/ms)	.16 ± .02	.17 ± .03	< .0001
1st Applanation Time (A1 Time) (ms)	7.19 ± .28	7.00 ± .28	< .0001
A1 Deflection Amplitude (A1 DeflAmp) (mm)	.09 ± .01	.10 ± .02	< .0001
Deformation Amplitude Ratio (DA Ratio) (unitless)	4.37 ± .42	5.81 ± .1.38	< .0001
Deflection Amplitude Ratio (DeflA Ratio) (unitless)	5.06 ± .65	7.16 ± 4.82	< .0001
Deformation Amplitude (DA) (mm)	1.09 ± .10	1.18 ± .12	< .0001
HCDeflAmp (mm)	.91 ± .11	1.01 ± .13	< .0001
HCDeflArea (mm^2)	3.39 ± .55	3.54 ± ..53	0.013
HCdarclength (mm)	-.14 ± .02	-.12 ± .03	< .0001
Peak Distance (mm)	5.08 ± .26	5.05 ± .24	0.226
HC Radius of Concave Curvature (HC Radius) (mm)	7.08 ± .79	5.62 ± 1.00	< .0001
Maximum Inverse Radius (InvRadMax) (1/mm)	.168 ± .02	.22 ± .04	< .0001
Maximum Whole Eye Motion (WEM Max)(mm)	.29 ± .07	.27 ± .06	0.0065
2nd Applanation Length (A2 Length) (mm)	1.73 ± .31	1.53 ± .41	< .0001
2nd Applanation Velocity (A2 Vel) (mm/ms)	-.40 ± .08	-.47 ± .11	< .0001
2nd Applanation Time (A2 Time) (ms)	21.78 ± .37	21.96 ± .39	< .0001
Stiffness Parameter, SP-A1 (mmHg/mm)	108.10 ± 20.52	68.67 ± 23.64	<.0001
Stiffness Parameter, SP-HC (mmHg/mm)	12.09 ± 3.75	7.63 ± 3.27	<.0001

1st Applanation = A1
HC = Highest Concavity
Note: In DeflA Ratio, one KC eye was excluded as an outlier.

Table 2: Regression Analysis Statistics between Stiffness Parameter SP-A1 and Dynamic Corneal Response Parameters

	Normal (N = 482)	**Keratoconus (N = 180)**	**Slope NL,KC**
Pachymetry (µm)	R^2 = 0.2213; p < .0001	R^2 = 0.2266; p < .0001	+, +
A1 Length (mm)	p = 0.81	R^2 = 0.0434; p = 0.006	0, +
A1 Vel (mm/ms)	R^2 = 0.3312; p < .0001	R^2 = 0.1586; p < .0001	-, -
A1 Time (ms)	R^2 = 0.4270; p < .0001	R^2 = 0.3771; p < .0001	+, +
A1 DeflAmp (mm)	p = 0.98	R^2 = 0.1347; p < .0001	0, -
DA Ratio (unitless)	R^2 = 0.2914; p < .0001	R^2 = 0.3179; p < .0001	-, -
DA (mm)	R^2 = 0.3253; p < .0001	R^2 = 0.4833; p < .0001	-, -
HCDeflAmp (mm)	R^2 = 0.3331; p < .0001	R^2 = 0.4973; p < .0001	-, -
HCDeflArea (mm^2)	R^2 = 0.2982; p < .0001	R^2 = 0.3618; p < .0001	- , -
HCdarclength (mm)	R^2 = 0.0294; p = 0.0002	R^2 = 0.0561; p = 0.0017	+, -
Peak Distance (mm)	R^2 = 0.2771; p < .0001	R^2 = 0.1952; p < .0001	-, -
HC Radius (mm)	R^2 = 0.0767; p < .0001	R^2 = 0.2802; p < .0001	+, +
InvRadMax (1/mm)	R^2 = 0.1206; p < .0001	R^2 =0.3319; p < .0001	-, -
WEM Max (mm)	p = 0.09	p = 0.36	0, 0
A2 Length (mm)	R^2 = 0.0530; p < .0001	R^2 =0.0683; p = 0.0005	+, +
A2 Vel (mm/ms)	R^2 = 0.3082; p < .0001	R^2 =0.3142; p < .0001	+, +
A2 Time (ms)	R^2 = 0.2631; p < .0001	R^2 =0.1852; p < .0001	-, -

Table 3: Regression Analysis Statistics between Stiffness Parameter SP-HC and Dynamic Corneal Response Parameters

	Normal (N = 482)	**Keratoconus (N = 180)**	**Slope KC,NL**
Pachymetry (µm)	R^2 = 0.2070; p < .0001	R^2 = 0.1760; p < .0001	+, +
A1 Length (mm)	R^2 = 0.0210; p = 0.002	R^2 = 0.0522; p = 0.003	+, +
A1 Vel (mm/ms)	R^2 = 0.2685; p < .0001	R^2 = 0.0554; p = 0.002	-, -
A1 Time (ms)	R^2 = 0.6280; p < .0001	R^2 = 0.5726; p < .0001	+, +
A1 DeflAmp (mm)	R^2 = 0.2103; p < .0001	p = 0.84	+, 0
DA Ratio (unitless)	R^2 = 0.2398; p < .0001	R^2 = 0.2357; p < .0001	-, -
DA (mm)	R^2 = 0.5112; p < .0001	R^2 = 0.5268; p < .0001	-, -
HCDeflAmp (mm)	R^2 = 0.6184; p < .0001	R^2 = 0.5654; p < .0001	-, -
HCDeflArea (mm^2)	R^2 = 0.5610; p < .0001	R^2 = 0.4771; p < .0001	-, -
HCdarclength (mm)	R^2 = 0.0620; p < .0001	R^2 = 0.0243; p = .041	+, -
Peak Distance (mm)	R^2 = 0.6320; p < .0001	R^2 = 0.3899; p < .0001	-, -
HC Radius (mm)	R^2 = 0.1095; p < .0001	R^2 = 0.2084; p < .0001	+, +
InvRadMax (1/mm)	R^2 = 0.0923; p < .0001	R^2 = 0.2213; p < .0001	-,-
WEM Max (mm)	R^2 = 0.0334; p < .0001	p = 0.46	+, 0
A2 Length (mm)	R^2 = 0.0936; p < .0001	R^2 = 0.0596; p = 0.001	+, +
A2 Vel (mm/ms)	R^2 = 0.5028; p < .0001	R^2 = 0.3197; p < .0001	+, +
A2 Time (ms)	R^2 = 0.3248; p < .0001	R^2 = 0.2911; p < .0001	-, -

Figure 1: **A**: Experimental set up for hot wire anemometry; and **B**: Locations for measurement of air puff velocity relative to nozzle.

Figure 2: **A**: Measured velocity (red) and Corvis-exported pressure signal (green), both time-synchronized by the photo cell signal (blue) **B**: Centerline Velocity Distribution as a function of distance from the nozzle.

Figure 3: Regression analysis of HCdarlength vs HCDeflAmp. Note the significant but opposite relationships of both NL and KC groups. In NL eyes, as HC Deflection amp increases, the negative magnitude of delta arclength also increases. In other words, the greater the resistance to deformation (low HCDeflAmp), the less the acrlength shortened. However, the KC eyes had less shortening of the arclength, even with greater HC Deflection amp, likely due to pathology of the collagen fibers, limiting normal folding with arclength shortening.

Figure 4: Regression analysis of A) Pachymetry vs Stiffness Parameter, SP-A1; and B) Pachymetry vs SP-HC, both showing that thicker corneas tend to be stiffer in both NL (black) and KC (red) eyes. Note that SP-A1 shows greater separation between keratoconic eyes and normal eyes.

Figure 5: Regression analysis of A) DA Ratio 2mm vs Stiffness Parameter, SP-A1; and B) DA Ratio 2mm vs SP-HC, both showing that stiffer eyes with greater resistance to deformation have lower magnitude DA Ratio in both NL (black) and KC (red) eyes. Note that SP-A1 shows greater separation between keratoconic eyes and normal eyes.

Figure 6: Regression analysis of A) DeflAmpMax vs Stiffness Parameter, SP-A1; and B) DeflAmpMax vs SP-HC, both showing stiffer eyes have lower maximum corneal deflection in both NL (black) and KC (red) eyes.

Figure 7: Regression analysis of A) HC Radius vs Stiffness Parameter, A-1; and B) HC Radius vs SP-HC, both showing stiffer eyes have greater radius of concave curvature or are flatter at highest concavity in both NL (black) and KC (red) eyes.

A

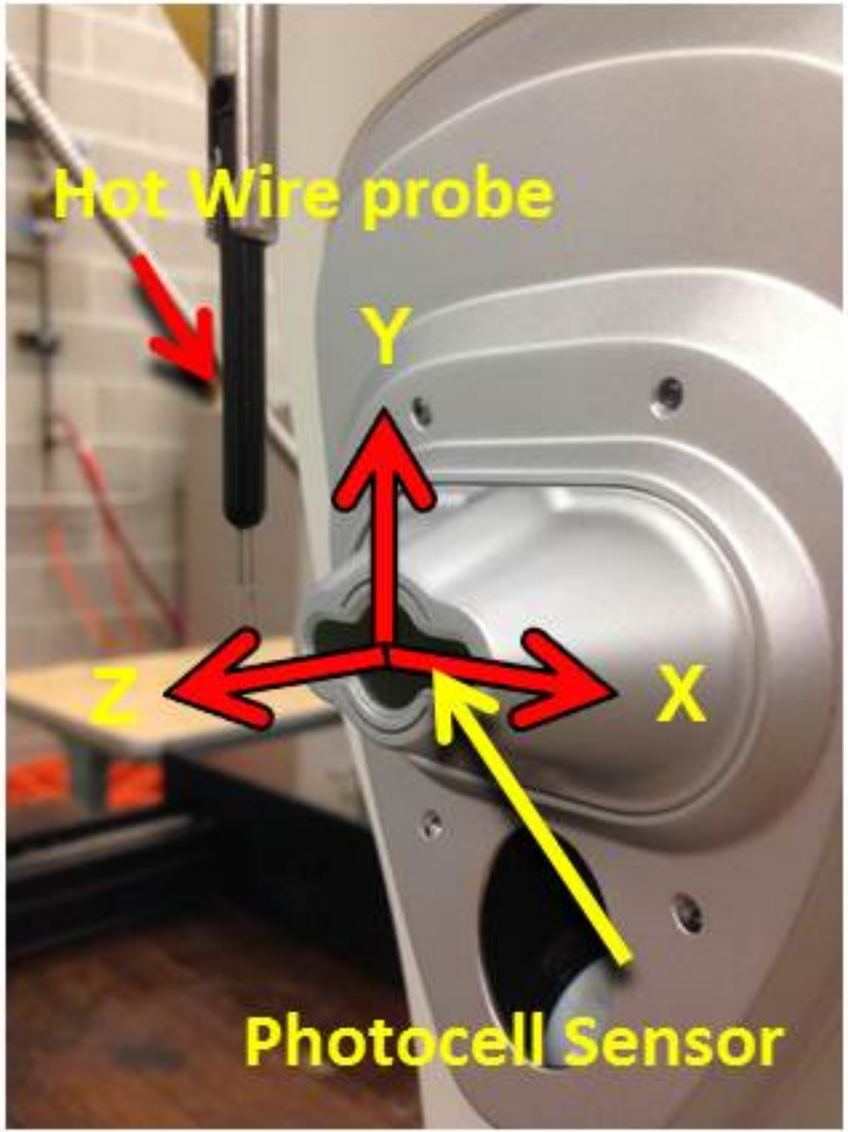

B

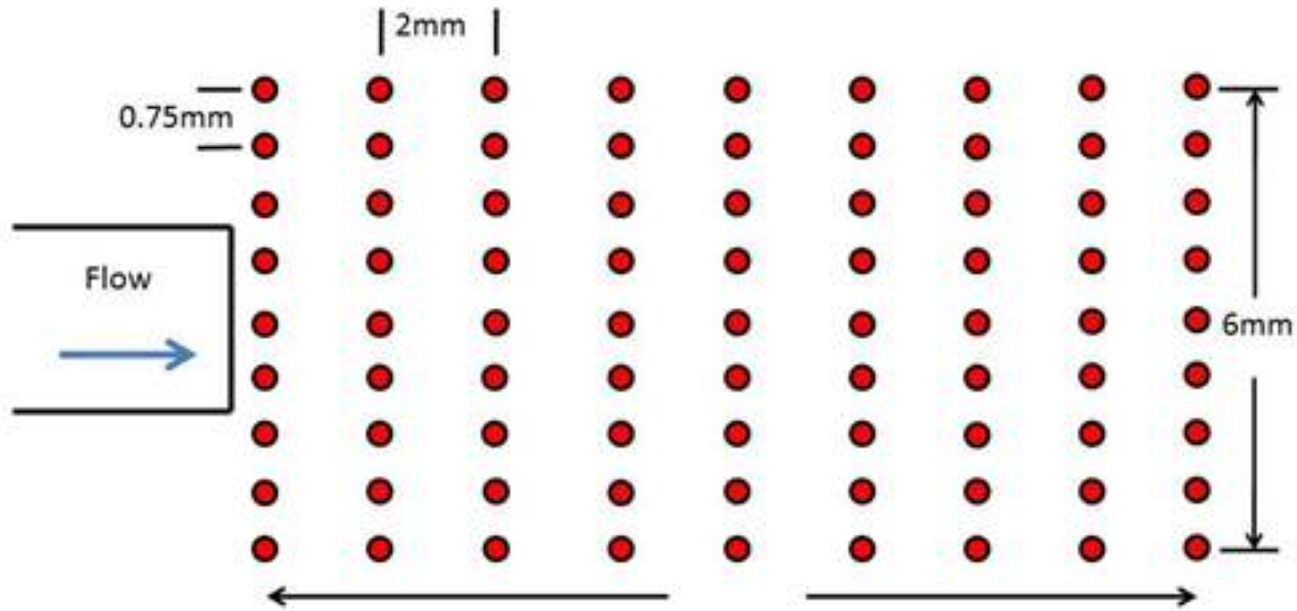

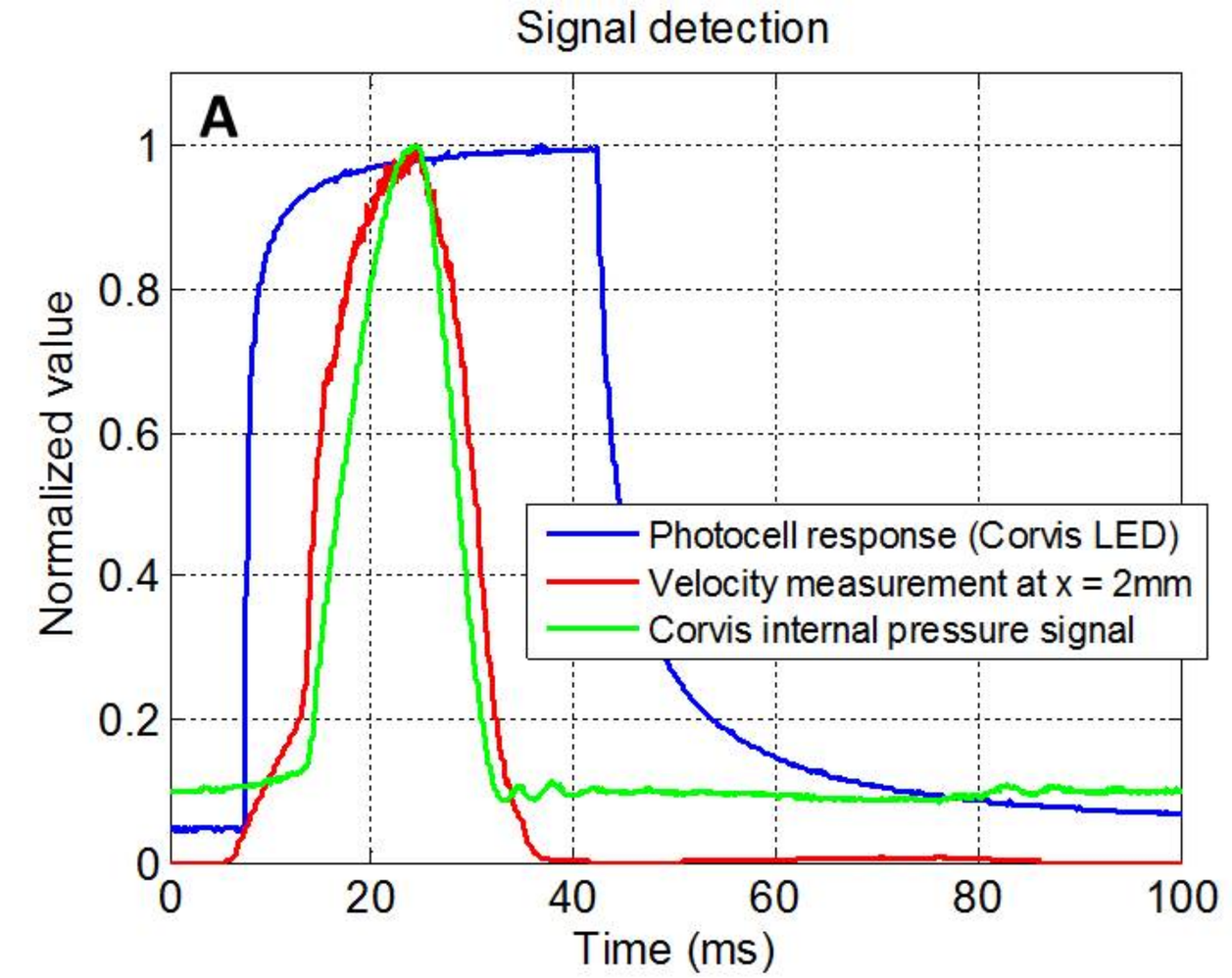
Signal detection
A
Normalized value
Time (ms)
Photocell response (Corvis LED)
Velocity measurement at x = 2mm
Corvis internal pressure signal

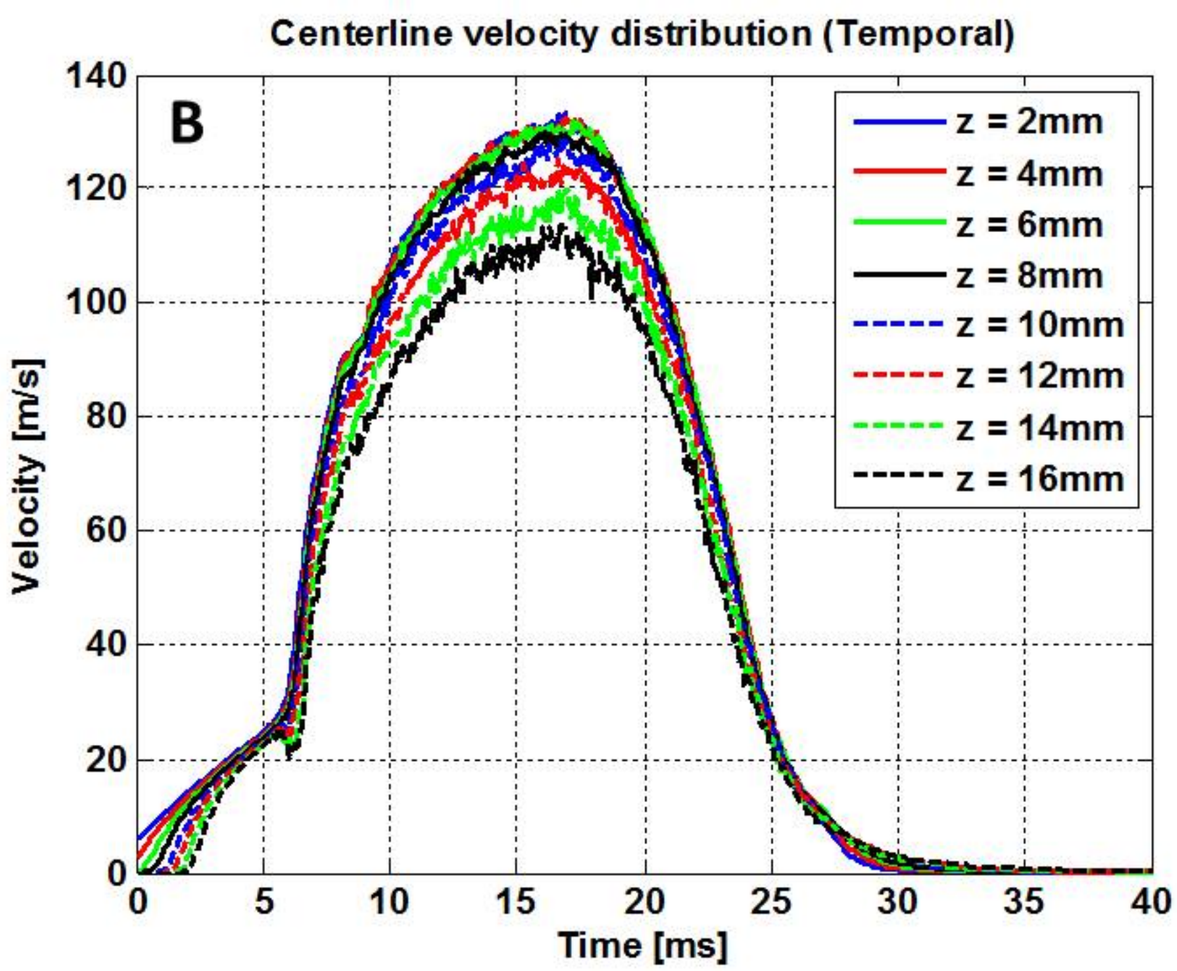
Centerline velocity distribution (Temporal)
B
Velocity [m/s]
Time [ms]
z = 2mm
z = 4mm
z = 6mm
z = 8mm
z = 10mm
z = 12mm
z = 14mm
z = 16mm

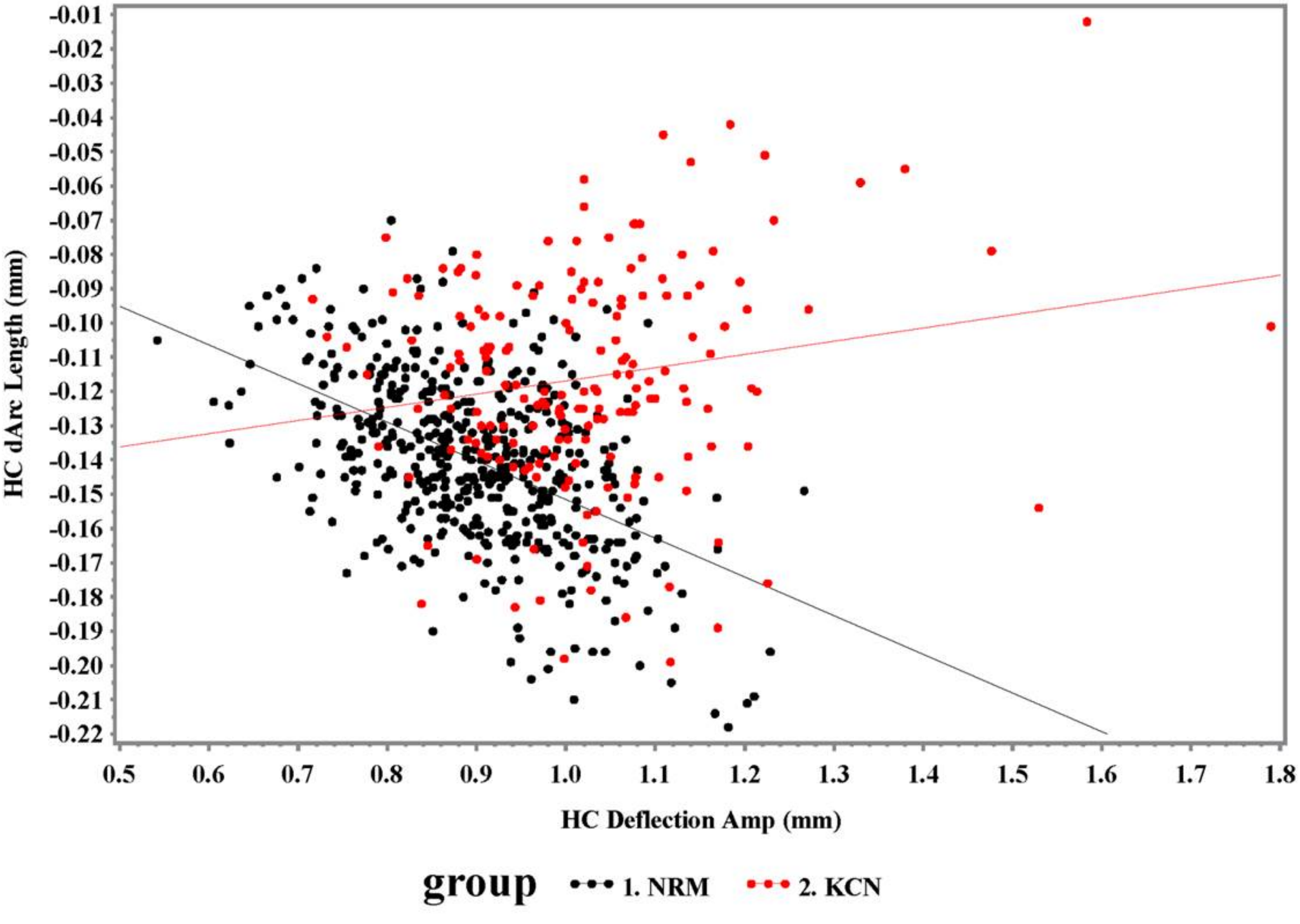
HC dArc Length (mm)
-0.01
-0.02
-0.03
-0.04
-0.05
-0.06
-0.07
-0.08
-0.09
-0.10
-0.11
-0.12
-0.13
-0.14
-0.15
-0.16
-0.17
-0.18
-0.19
-0.20
-0.21
-0.22
0.5
0.6
0.7
0.8
0.9
1.0
1.1
1.2
1.3
1.4
1.5
1.6
1.7
1.8
HC Deflection Amp (mm)
group
1. NRM
2. KCN

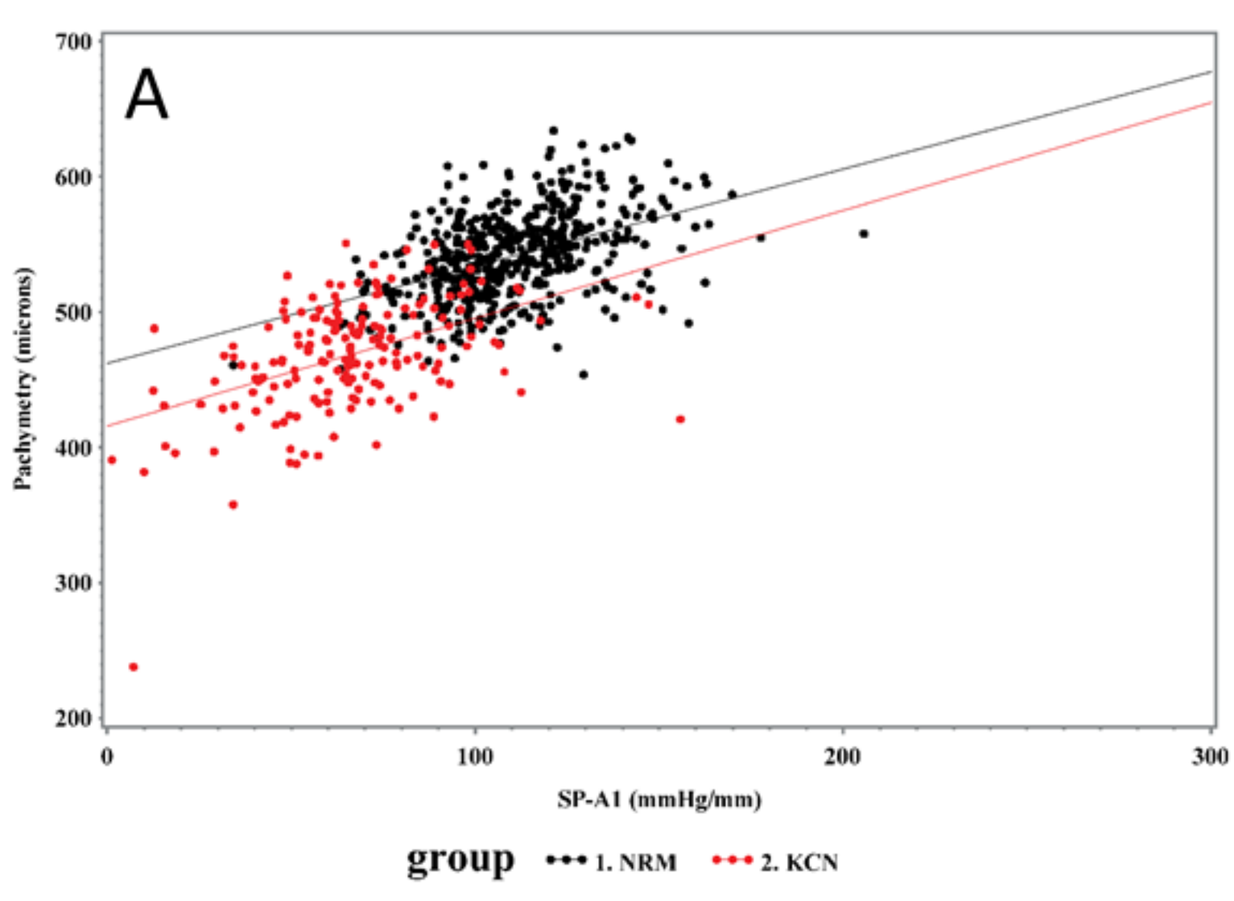
A
Pachymetry (microns)
700
600
500
400
300
200
0
100
200
300
SP-A1 (mmHg/mm)
group
1. NRM
2. KCN

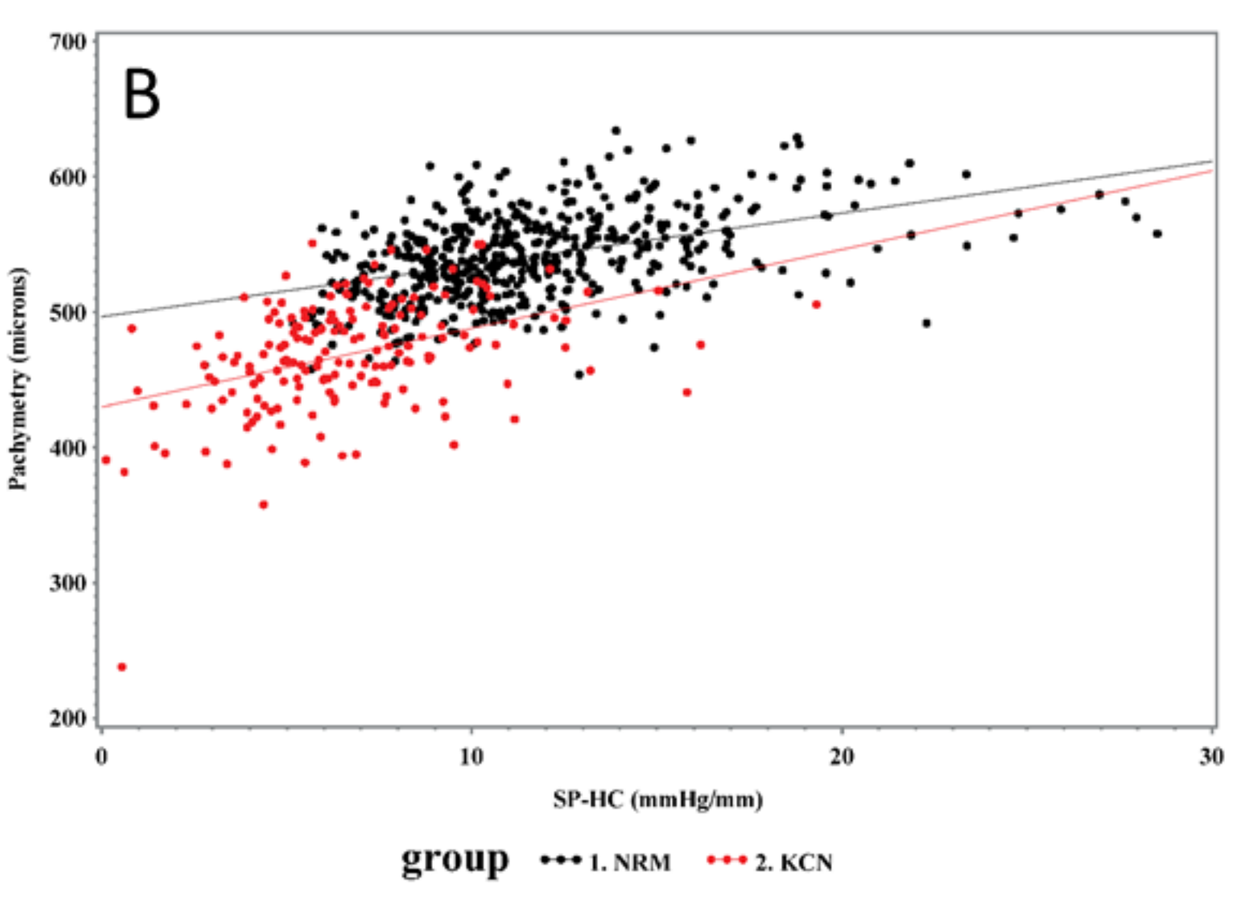
B
Pachymetry (microns)
700
600
500
400
300
200
0
10
20
30
SP-HC (mmHg/mm)
group
1. NRM
2. KCN

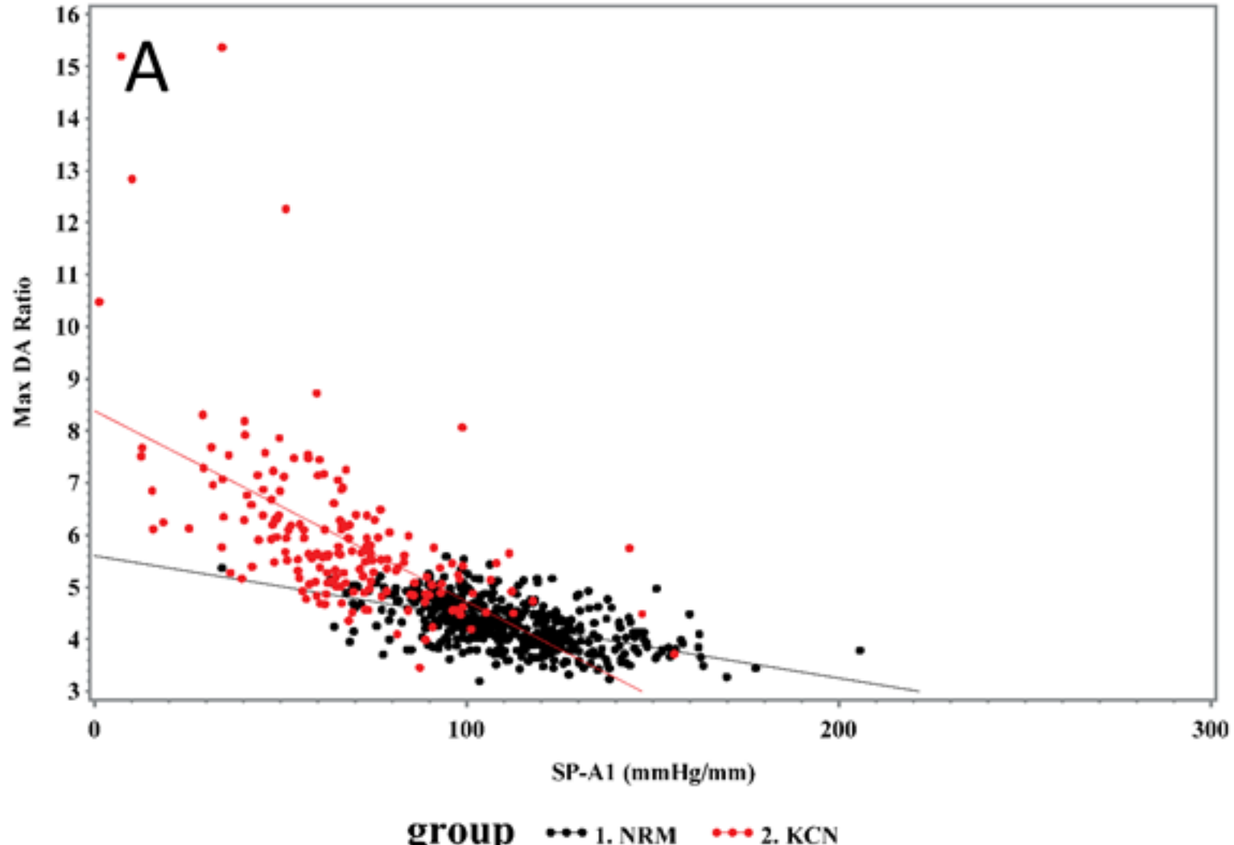
A
Max DA Ratio
SP-A1 (mmHg/mm)
group
1. NRM
2. KCN

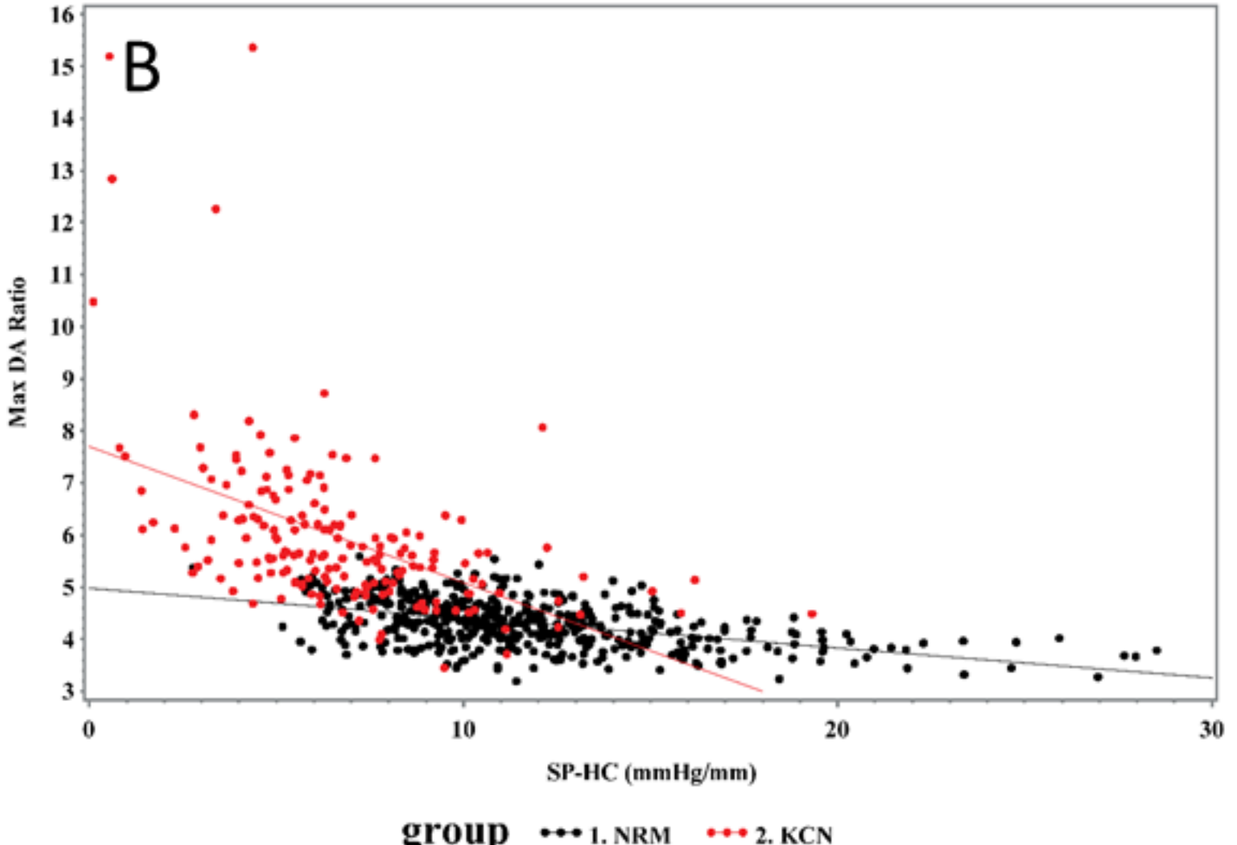
B
Max DA Ratio
SP-HC (mmHg/mm)
group
1. NRM
2. KCN

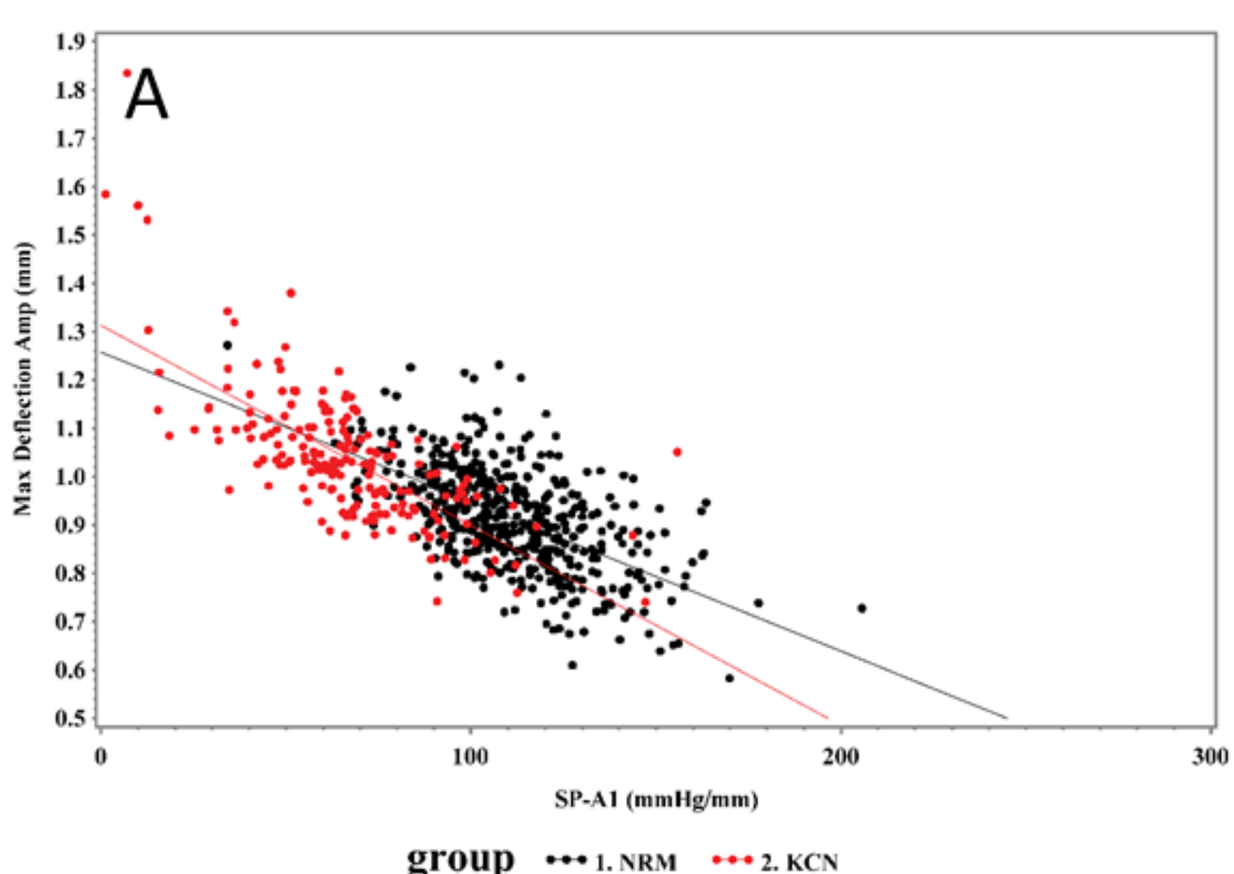
A
Max Deflection Amp (mm)
1.9
1.8
1.7
1.6
1.5
1.4
1.3
1.2
1.1
1.0
0.9
0.8
0.7
0.6
0.5
0
100
200
300
SP-A1 (mmHg/mm)
group
1. NRM
2. KCN

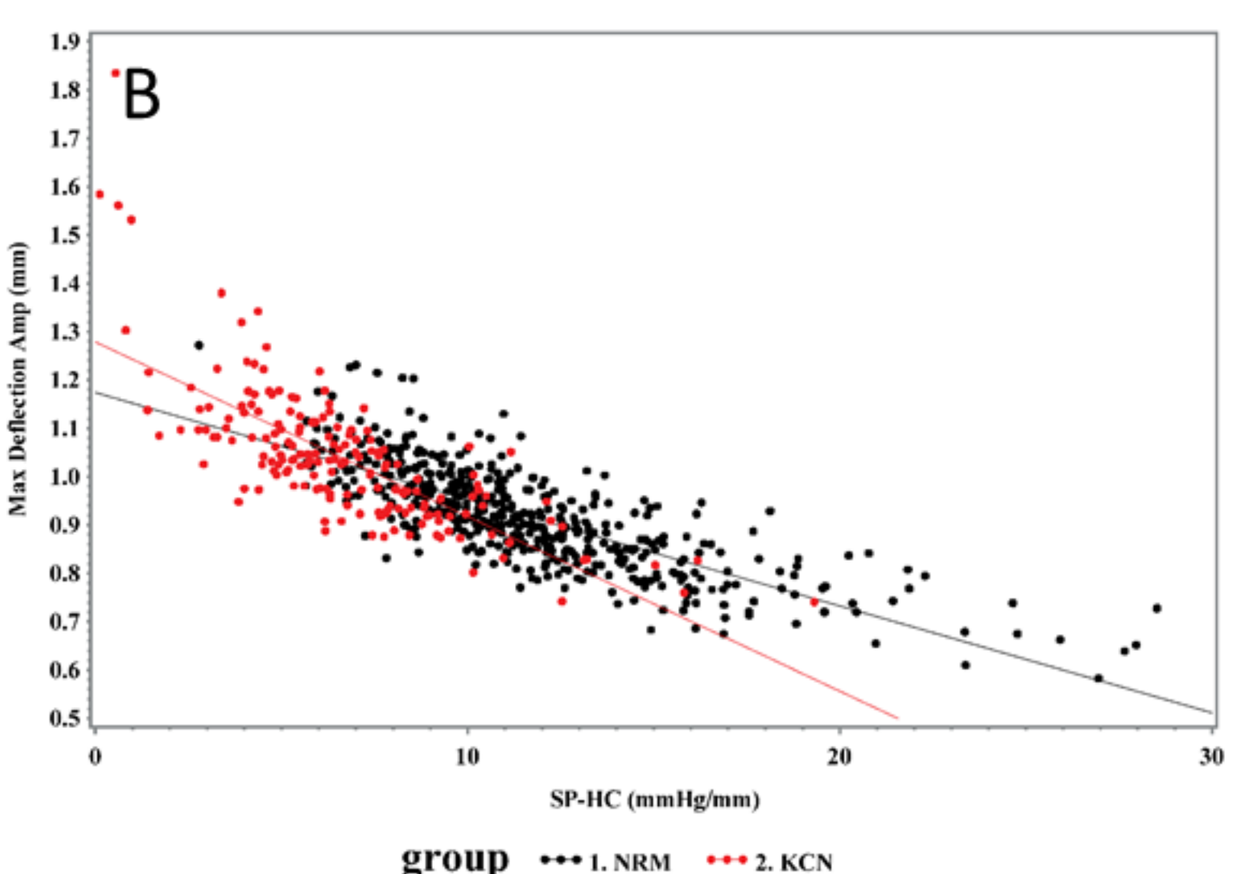
B
Max Deflection Amp (mm)
1.9
1.8
1.7
1.6
1.5
1.4
1.3
1.2
1.1
1.0
0.9
0.8
0.7
0.6
0.5
0
10
20
30
SP-HC (mmHg/mm)
group
1. NRM
2. KCN

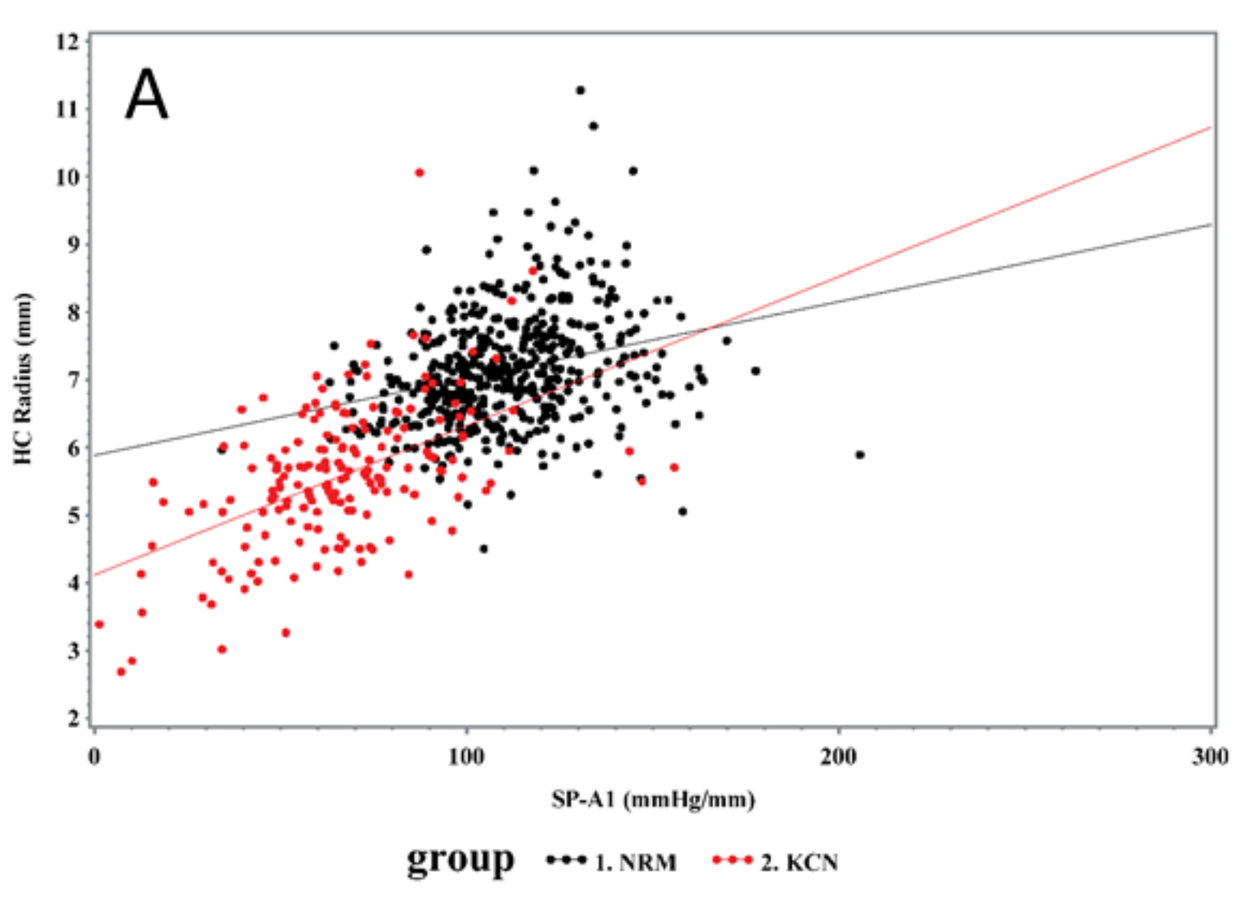
A
HC Radius (mm)
SP-A1 (mmHg/mm)
group
1. NRM
2. KCN

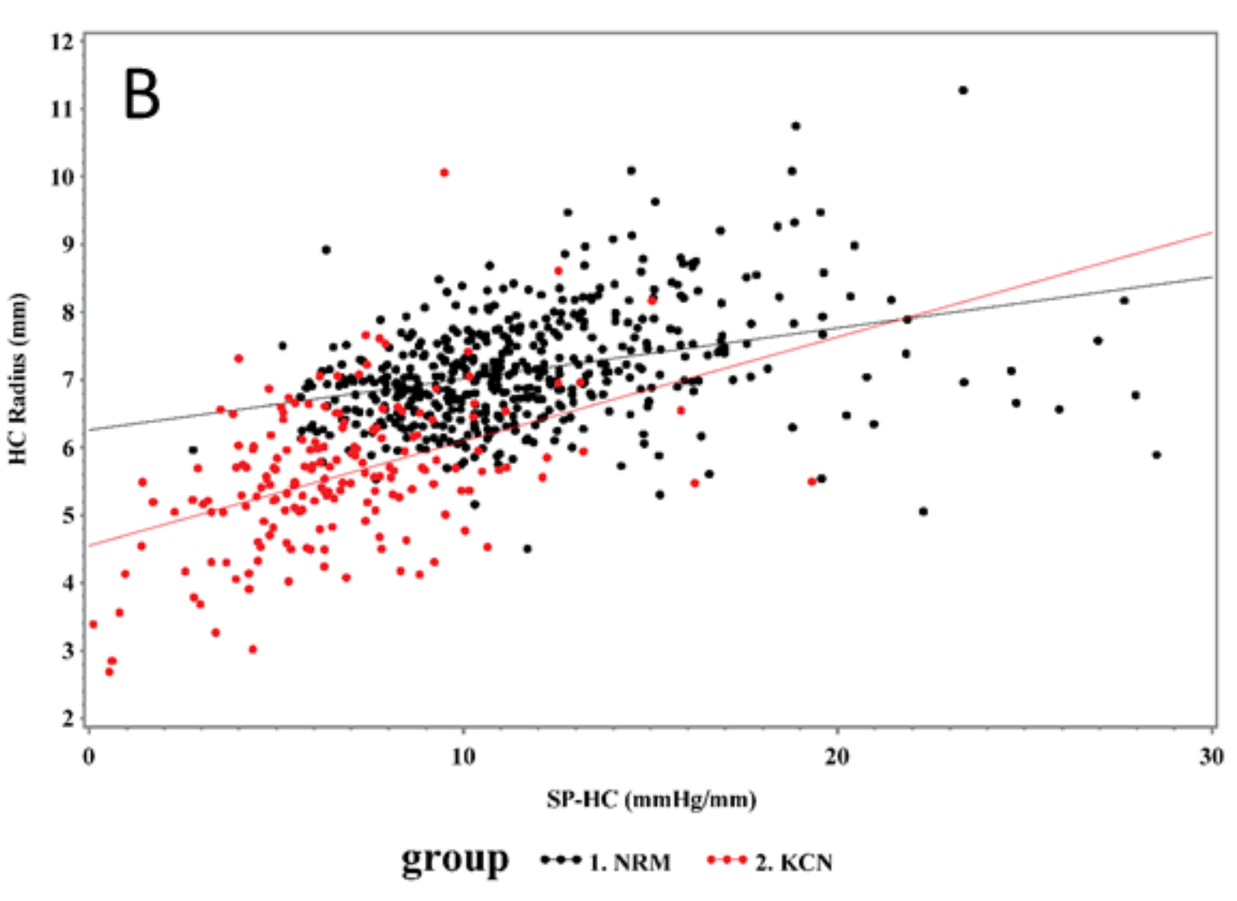
B
HC Radius (mm)
SP-HC (mmHg/mm)
group
1. NRM
2. KCN